THE ASTROPHYSICAL JOURNAL, 615:L37–L40, 2004 November 1

DOES AN NeNa CYCLE EXIST IN EXPLOSIVE HYDROGEN BURNING?

C. ROWLAND,[1,2,3] C. ILIADIS,[1,2] A. E. CHAMPAGNE,[1,2] C. FOX,[1,2] J. JOSÉ,[1,4] AND R. RUNKLE[1,2]

Received 2004 August 11; accepted 2004 September 15; published 2004 September 21

ABSTRACT

According to common assumptions, matter in the mass range $A \geq 20$ is processed through the so-called NeNa cycle during hydrogen-burning nucleosynthesis. The existence of such a reaction cycle implies that the (p, α) reaction on ^{23}Na is more likely to occur than the competing (p, γ) reaction. However, recently evaluated thermonuclear rates for both reactions carry relatively large uncertainties and allow for both possibilities, i.e., a "closed" and an "open" NeNa cycle. We measured the ^{23}Na$(p, \gamma)^{24}$Mg reaction at the Laboratory for Experimental Nuclear Astrophysics. The present experimental results, obtained with our sensitive γ-ray detection apparatus, reduce the ^{23}Na + p reaction rate uncertainties significantly. We demonstrate that a closed NeNa cycle does not exist at stellar temperatures of $T = 0.2$–0.4 GK. The new results have important implications for the nucleosynthesis in classical novae, including the amount of ^{26}Al ejected by the thermonuclear explosion, the elemental abundances of Mg and Al observed in nova shells, and observations of Mg and Al isotopic ratios in primitive meteorites.

Subject headings: novae, cataclysmic variables — nuclear reactions, nucleosynthesis, abundances — stars: abundances

1. INTRODUCTION

During hydrogen burning in the mass $A \geq 20$ region, the nucleosynthesis path is likely to reach the isotope ^{23}Na. Two possibilities exist for subsequent nuclear processing, either through the ^{23}Na$(p, \alpha)^{20}$Ne reaction or via ^{23}Na$(p, \gamma)^{24}$Mg. The former reaction transforms ^{23}Na to a lighter isotope (^{20}Ne) and thereby gives rise to the so-called NeNa cycle (Rolfs & Rodney 1988). The competing (p, γ) reaction, on the other hand, transforms ^{23}Na to heavier isotopes and, hence, bypasses the NeNa cycle. The obvious question of interest for the nucleosynthesis path is how much material is processed through the (p, α) reaction on ^{23}Na as opposed to the competing (p, γ) reaction. The most important quantity in this regard is the reaction rate branching ratio, i.e., the ratio of thermonuclear rates for the ^{23}Na(p, α) and ^{23}Na(p, γ) reactions, $B_{p\alpha/p\gamma} = N_A\langle\sigma v\rangle_{p\alpha}/N_A\langle\sigma v\rangle_{p\gamma}$. A ratio greater than unity, $B_{p\alpha/p\gamma} > 1$, implies substantial NeNa cycling, while a ratio of $B_{p\alpha/p\gamma} \leq 1$ indicates that a closed NeNa cycle does not exist.

Figure 1 shows for stellar temperatures of $T = 0.1$–1.0 GK the ratio $B_{p\alpha/p\gamma}$, obtained by using the ^{23}Na + p reaction rates from the NACRE compilation (Angulo et al. 1999). The dashed line corresponds to the ratio of recommended rates, while the solid lines represent the corresponding errors. It can be seen that the branching ratio varies by 4 orders of magnitude at $T = 0.1$ GK and by 1 order of magnitude at $T = 0.3$ GK. Interestingly, the reaction rate errors allow for both possibilities, $B_{p\alpha/p\gamma} \leq 1$ and $B_{p\alpha/p\gamma} > 1$. Hence, based on the reaction rate errors shown in Figure 1, it is not possible to make an unambiguous statement regarding the existence of a closed NeNa cycle at elevated stellar temperatures ($T \geq 0.1$ GK). Therefore, we suspect that the uncertainty in ^{23}Na + p reaction rates will have a significant influence on the nucleosynthesis in the mass $A \geq 20$ range during explosive hydrogen burning. This conclusion is supported by results of a recent reaction rate sensitivity study (Iliadis et al. 2002).

The errors shown in Figure 1 are mainly caused by an unobserved narrow resonance. This case represents an example in nuclear astrophysics when a single resonance dominates the reaction rates. The resonance corresponds to a known state at $E_X = 11{,}830.7 \pm 1.5$ keV (Endt 1990; Hale et al. 2004) in the ^{24}Mg compound nucleus. Its expected location is $E_R^{\rm lab} \approx 144$ keV, as calculated from the excitation energy and the proton separation energy in ^{24}Mg ($S_p = 11{,}692.68 \pm 0.01$ keV; Audi et al. 2003). The previously reported upper limits for the (p, γ) and (p, α) resonance strengths amount to $\omega\gamma_{p\gamma} \leq 5 \times 10^{-6}$ eV and $\omega\gamma_{p\alpha} \leq 5 \times 10^{-7}$ eV, respectively (Görres et al. 1989). In this Letter, we report on a new search for this unobserved resonance in the ^{23}Na$(p, \gamma)^{24}$Mg reaction. In § 2, we discuss the experimental setup and present our new experimental results. In § 3, we describe hydrodynamic simulations of classical novae in order to investigate the astrophysical impact of our new reaction rates. It is shown that our results have important implications for the synthesis of magnesium and aluminum in classical novae, in particular for the radioisotope ^{26}Al.

2. EXPERIMENTAL SETUP AND RESULTS

The experiment was carried out at the Laboratory for Experimental Nuclear Astrophysics, located at the Triangle Universities Nuclear Laboratory. A 1 MV Van de Graaff accelerator provided proton beams at laboratory energies between 130 and 450 keV, with beam currents of up to 100 μA on target. The target was directly water-cooled using deionized water. The target backing consisted of a 0.5 mm thick tantalum sheet. Prior to target preparation, the surface of the tantalum backing was etched in order to remove some of the impurities that are a source of beam-induced background radiation. The target itself was prepared by evaporating Na_2WO_4 onto the tantalum backing. The target was checked frequently by measuring the well-known $E_R^{\rm lab} = 309$ keV resonance in ^{23}Na$(p, \gamma)^{24}$Mg (Endt 1990). No degradation in yield or target thickness was observed during the course of the experiment. Prompt γ-rays from the ^{23}Na$(p, \gamma)^{24}$Mg

[1] Department of Physics and Astronomy, University of North Carolina, Chapel Hill, NC 27599-3255.

[2] Triangle Universities Nuclear Laboratory, P. O. Box 90308, Durham, NC 27708-0308.

[3] Current address: Naval Research Laboratory, Space Sciences Division, Code 7650, Washington, DC 20375.

[4] Departament de Física i Enginyeria Nuclear, Universitat Politecnica de Catalunya, Avenida Victor Balguer s/n, 08800 Vilanova i la Geltru, Barcelona; and Institut d'Estudis Espacials de Catalunya, E-08034 Barcelona, Spain.

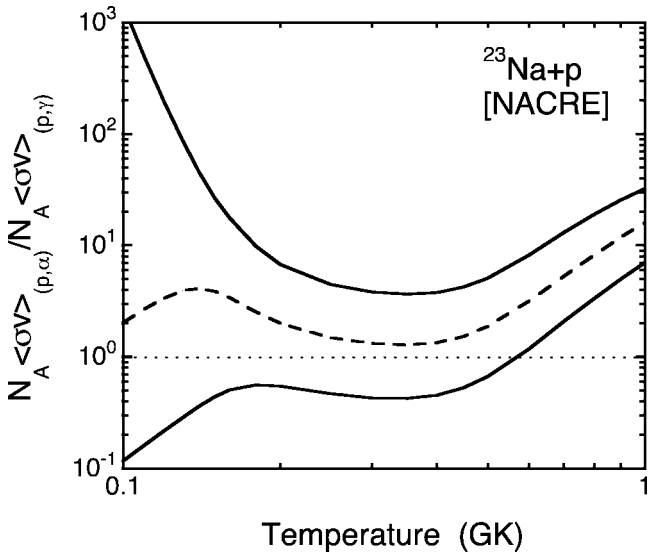

FIG. 1.—Ratio of ^{23}Na(p, α) and ^{23}Na(p, γ) reaction rates (Angulo et al. 1999) prior to the present work (*dashed line*: ratio of recommended rates; *solid lines*: corresponding uncertainties). The area between the solid lines represents the uncertainty in the reaction rate ratio.

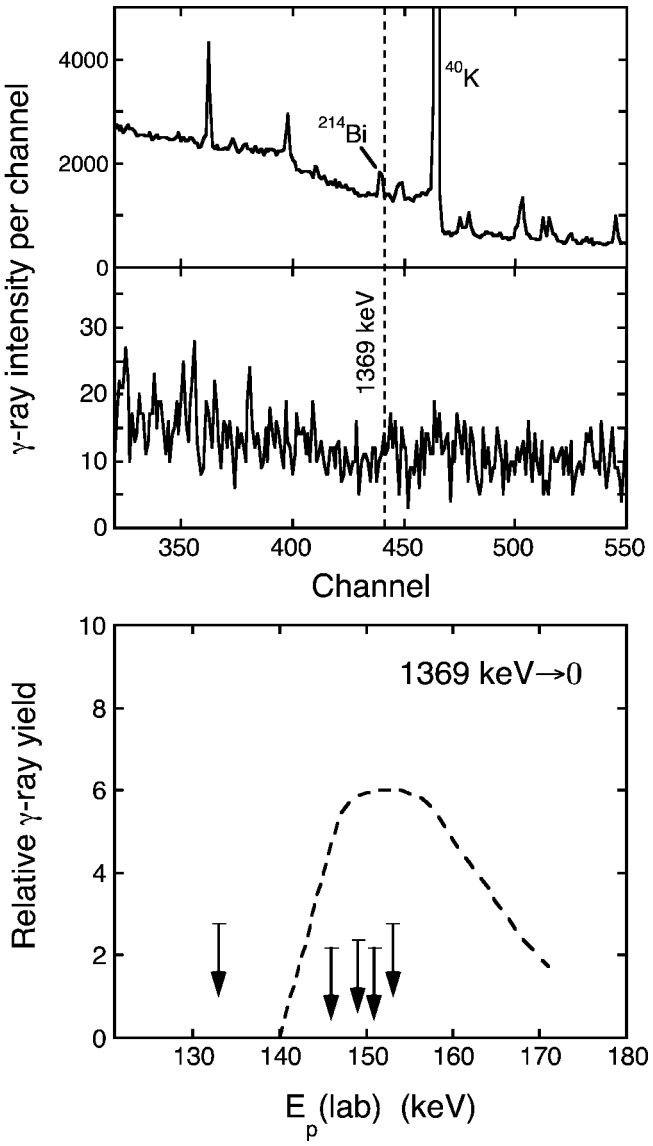

FIG. 2.—*Top*: Singles HPGe detector γ-ray spectrum, measured in the ^{23}Na(p, γ)^{24}Mg reaction at $E_p^{\rm lab} = 150$ keV. The accumulated charge amounts to ≈6 C. The location of the expected 1369 keV → 0 transition in ^{24}Mg is indicated by the vertical dashed line. All visible peaks originate from well-known room-background contributions. *Middle*: Corresponding coincidence HPGe detector γ-ray spectrum, obtained with the condition 3 MeV < $E_\gamma^{\rm HPGe} + E_\gamma^{\rm NaI(Tl)}$ < 13 MeV for the sum of HPGe and NaI(Tl) detector energies. The γ-ray background is significantly reduced by the coincidence requirement. *Bottom*: Excitation function for the intensity of the 1369 keV → 0 transition in ^{24}Mg. The dashed line, showing the shape of the expected yield curve of the unobserved $E_R^{\rm lab} = 144$ keV resonance, is obtained by correcting the target profile over the well-known $E_R^{\rm lab} = 309$ keV resonance for the ratio of effective proton stopping powers. The target thickness amounts to ≈23 keV at $E_p^{\rm lab} = 144$ keV.

reaction were detected using an apparatus consisting of two detectors. A large-volume (582 cm^3) high-purity germanium (HPGe) detector, placed at an angle of 0° and at a distance of 16 mm from the target, acted as a primary counter. The secondary counter consisted of an NaI(Tl) annular detector with an outer diameter, inner diameter, and crystal length of 36, 12, and 36 cm, respectively. Both the target chamber and the HPGe detector crystal were placed inside the NaI(Tl) counter, with the target located near the center of the annulus. Energy and efficiency calibrations were established using radioactive sources and the decays from well-known resonances in the ^{14}N(p, γ)^{15}O and ^{27}Al(p, γ)^{28}Si reactions. In our measuring geometry, the NaI(Tl) annulus acted both as a coincidence counter as well as an anticoincidence (i.e., antimuon) shield, depending on the γ-ray transition under consideration. The use of two γ-ray detectors in coincidence and/or anticoincidence significantly reduces the γ-ray background in our spectra, as will be shown below. A detailed account of this technique is given in Rowland et al. (2002).

Some of our experimental results are shown in Figure 2. The top part displays γ-ray spectra measured at a bombarding proton energy of $E_p^{\rm lab} = 150$ keV, i.e., in the region of the unobserved $E_R^{\rm lab} = 144$ keV resonance. The top panel shows an HPGe detector "singles" (without any coincidence requirement) spectrum. The location of the expected $E_\gamma = 1369$ keV γ-ray from the decay of the first excited state in the compound nucleus ^{24}Mg is indicated by the vertical dashed line. The peak visible to the left of the dashed line does not originate from transitions in ^{24}Mg but represents a well-known room-background contribution from ^{214}Bi. The large background obscures any expected signal. The middle panel displays the HPGe detector coincidence spectrum that is obtained by gating on a specific region (3 MeV < $E_\gamma^{\rm HPGe} + E_\gamma^{\rm NaI(Tl)}$ < 13 MeV) in the two-dimensional histogram of HPGe versus NaI(Tl) detector energies. The lower threshold of 3 MeV rejects room-background events (e.g., from ^{40}K and ^{208}Tl), while the upper threshold of 13 MeV reduces unwanted high-energy events (e.g., induced by cosmic-ray muons). It can be seen that the γ-ray background in the coincidence spectrum is suppressed by orders of magnitude. Since the coincidence requirement reduces the overall detection efficiency only by a factor of ≈2, the signal-to-noise ratio is significantly improved. The expected $E_\gamma = 1369$ keV γ-ray is still not visible in the coincidence spectrum. Our measured excitation function (i.e., γ-ray yield vs. bombarding proton energy) for the intensity of the 1369 keV → 0 transition in the HPGe coincidence spectra is shown in the bottom panel of the figure. The dashed curve, representing the shape of the expected yield curve for the unobserved $E_R^{\rm lab} = 144$ keV resonance, is based on the known resonance location and the target profile over the well-known $E_R^{\rm lab} = 309$ keV resonance. In the range of $E_p = 130$–155 keV, the yield from the ^{23}Na(p, γ)^{24}Mg reaction was measured at

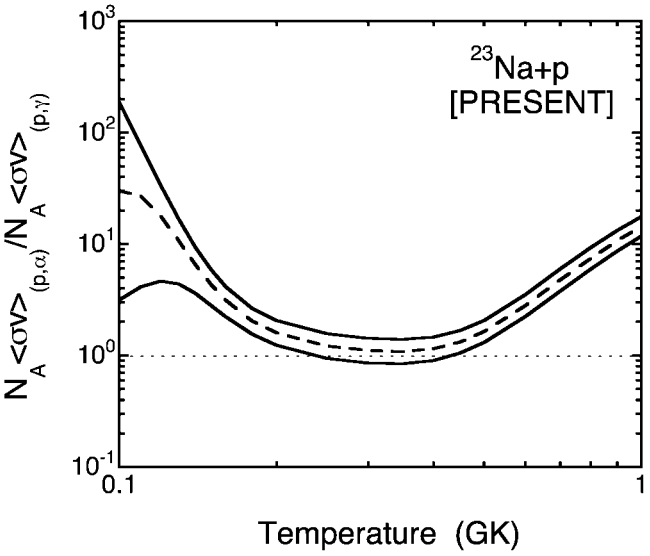

FIG. 3.—Same as Fig. 1, but with ^{23}Na + p rates from the present work. Comparison to Fig. 1 reveals the significant reduction in reaction rate ratio uncertainties due to the improved experimental upper limit for the (p, γ) strength of the E_R^{lab} = 144 keV resonance.

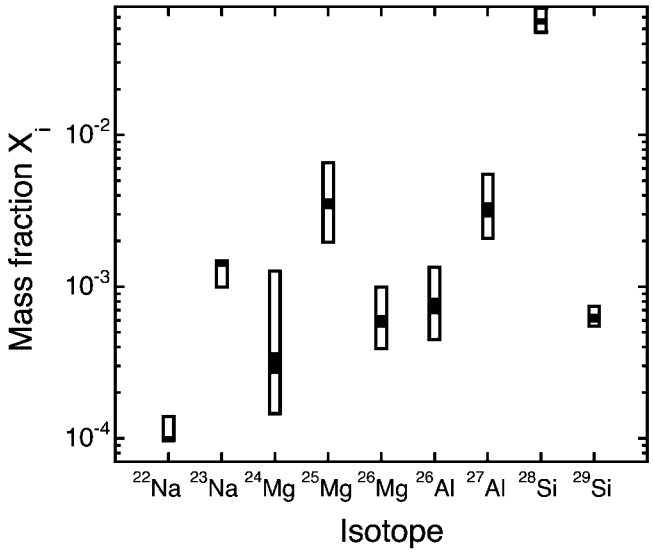

FIG. 4.—Mean ejected abundances (mass fractions) of Na, Mg, Al, and Si isotopes at the end of hydrodynamic nova model computations, i.e., when the expanding envelope has reached a radius of 10^{12} cm. The vertical bars represent the range of values that result from ^{23}Na(p, γ)^{24}Mg and ^{23}Na(p, α)^{20}Ne reaction rate uncertainties only. The open and filled bars are obtained by using the previous (Angulo et al. 1999) and present ^{23}Na + p reaction rates, respectively.

five energies, covering both the "on-resonance" and the "off-resonance" regions. No γ-rays from transitions in ^{24}Mg have been observed in any of our singles or coincidence spectra. Our new data allow for the estimation of an improved upper limit for the (p, γ) resonance strength. The result is $\omega\gamma_{p\gamma} \leq 1.5 \times 10^{-7}$ eV. This value includes the uncertainties in γ-ray detection efficiency (5%), beam current integration (5%), and adopted (J. F. Ziegler & J. P. Biersack 2000, unpublished) stopping powers (15%). Compared to the previously reported result (Görres et al. 1989), the upper limit of the $\omega\gamma_{p\gamma}$ value is reduced by a factor of 33. Using our new upper limit for $\omega\gamma_{p\gamma}$, together with the previously reported value of the branching ratio Γ_γ/Γ (Vermeer et al. 1988) for the E_X = 11,831 keV level in ^{24}Mg, we also obtain an improved estimate for the upper limit of the (p, α) resonance strength ($\omega\gamma_{p\alpha} \leq 1.5 \times 10^{-8}$ eV). Our procedure and analysis will be discussed in detail in a forthcoming publication (J. Newton et al. 2004, in preparation).

The new reaction rate branching ratio, $B_{p\alpha/p\gamma}$, is displayed in Figure 3. The dramatic improvement in accuracy compared to Figure 1 is evident. For example, at a stellar temperature of T = 0.3 GK, the present uncertainty in the branching ratio amounts to 30% compared to a factor of ≈3 in Figure 1. Our significantly improved ^{23}Na + p reaction rates allow more reliable statements regarding the nucleosynthesis path in the NeNa mass region. At T = 0.2–0.4 GK, the branching ratio $B_{p\alpha/p\gamma}$ is about unity; i.e., the (p, γ) reaction on ^{23}Na is as likely to occur as the competing (p, α) reaction. Each time when matter is processed through the NeNa reaction sequence, about 50% of material is lost from an NeNa cycle. Consequently, after a few such cycles, a relatively small fraction of matter remains stored in an NeNa cycle. The situation here is very different from the CNO cycles, where the values of $B_{p\alpha/p\gamma}$ at ^{15}N + p, ^{17}O + p, ^{18}O + p, and ^{19}F + p amount to 1000, 200, 300, and 4000, respectively (Angulo et al. 1999). We may conclude that a *closed* NeNa *cycle does not exist at stellar temperatures of* T = 0.2–0.4 GK. These considerations are important, for example, in classical novae since the peak temperatures predicted by current nova models fall within this temperature region (Kovetz & Prialnik 1997; Starrfield et al. 1998; José et al. 1999). At lower temperatures ($T \approx 0.1$ GK), a closed NeNa cycle is likely to develop. Similar conclusions hold for higher temperatures ($T \geq 0.6$ GK) but only if the nucleosynthesis path does not bypass ^{23}Na.

3. HYDRODYNAMIC SIMULATIONS OF CLASSICAL NOVAE

In order to investigate the influence of our new reaction rates on the nucleosynthesis in classical novae, we performed a series of hydrodynamic model simulations. A description of the hydrodynamic code SHIVA used for these simulations can be found in José & Hernanz (1998). We chose a nova model that assumes a 1.15 $M_\odot$ white dwarf of ONe composition, a mass accretion rate of 2×10^{-10} $M_\odot$ yr^{-1}, and 50% mixing between accreted and white dwarf matter prior to the outburst. This nova model achieves a peak temperature of T_{peak} = 0.23 GK (José et al. 1999). The only changes in the different nova model calculations concerned the choices of ^{23}Na(p, γ)^{24}Mg and ^{23}Na(p, α)^{20}Ne reaction rates. All allowed combinations of upper and lower limits of the ^{23}Na + p reaction rates have been taken into account. Note that none of the reaction-rate variations performed in the present work have a noticeable influence on the amount of hydrogen consumed, the amount of helium produced, or the total thermonuclear energy released. Variations of final isotopic abundances in the A = 20–30 mass range are displayed in Figure 4. The open and filled vertical bars represent the ranges of ejected mean mass fractions obtained by using the previously accepted (Angulo et al. 1999) and the present ^{23}Na + p rates, respectively. The improvement in the predicted values of final isotopic abundances is evident. In the following, we briefly discuss the main implications of our results.

First, the question regarding the Galactic origin of the radioisotope ^{26}Al is still unsolved. The recent detection of the Galactic ^{60}Fe γ-ray lines with the *RHESSI* satellite (Smith 2004) has revitalized this discussion. Whereas until recently Type II supernovae represented the most widely accepted production site of ^{26}Al, a new study (Prantzos 2004) suggests the need for an additional source. This has raised interest in Wolf-Rayet

stars and other production sites, such as classical novae. As shown in Figure 4, abundance predictions of ^{26}Al in classical novae are significantly affected by the large uncertainties in the previous ^{23}Na + p reaction rates (Angulo et al. 1999). Different combinations of upper and lower limits for the previous ^{23}Na(p, γ) and ^{23}Na(p, α) rates cause a variation in the ejected ^{26}Al mass fraction by a factor of ≈3. Using our new reaction rates, the variation is reduced to only 24%. Clearly, abundance predictions of ^{26}Al from hydrodynamic nova models are significantly improved.

Second, elemental magnesium and aluminum abundances have been observed in the shells of several classical novae (Warner 1995). These observations may significantly constrain hydrodynamic nova models but only if the predicted stellar model abundances show smaller variations as a result of uncertain nuclear physics input compared to the uncertainty of the observed abundance values. In our nova simulations, we find that the elemental Mg and Al mass fractions vary by factors of 3.4 and 2.6, respectively, if the previous ^{23}Na + p reaction rates are employed. Using the new rates, the variation amounts to less than 23% for both elements.

Third, the present study is also relevant for supporting the identification of presolar grains in primitive meteorites that originate from classical novae. Because of their small size, presolar oxide grains originating from novae have not been discovered yet. However, they are expected to condense in the ejected nova shells (see José et al. 2004) as spinel ($MgAl_2O_4$), corundum (Al_2O_3), or enstatite ($MgSiO_3$). If detected on Earth, these oxide grains will significantly constrain models of novae through their precisely measured oxygen, magnesium, and aluminum isotopic ratios. Our nova simulations predict rather robust values for the ratio of number abundances of ^{26}Al/^{27}Al ≈ 0.24, with a scatter of only a few percent as a result of previous or present ^{23}Na + p reaction rate uncertainties. However, the situation for the magnesium isotopes is quite different. Using the previous ^{23}Na + p reaction rates, we obtain variations of isotopic ratios in the ranges of ^{25}Mg/^{24}Mg = 6–13 and ^{26}Mg/^{24}Mg = 0.7–2.3. With the new reaction rates, we obtain rather precise values of ^{25}Mg/^{24}Mg = 11 and ^{26}Mg/^{24}Mg = 1.8, with variations amounting to less than 5%.

In summary, we demonstrated that a closed NeNa cycle does not exist in the stellar temperature range of T = 0.2–0.4 GK. Our experimental results significantly reduce the uncertainties in the abundances of magnesium and aluminum isotopes that are predicted by hydrodynamic simulations of classical novae. For illustrative purposes, only a single nova model is explored in the present work. Quantitative predictions regarding the contribution of classical novae to the amount of ^{26}Al detected in the Galaxy, the elemental Mg and Al abundances observed in nova ejecta, and interpretations of future measurements of Mg and Al isotopic ratios in presolar oxide grains of nova origin have to await the results of a more extensive numerical study involving a range of different nova models.

This work was supported in part by the US Department of Energy under contract DE-FG02-97ER41041, the Spanish MCYT grant AYA2004-06290-C02-02, and the Catalan AGAUR. J. J. would like to thank C. I. and A. E. C. for the kind hospitality during his sabbatical stay at the Department of Physics and Astronomy at the University of North Carolina at Chapel Hill.

REFERENCES

Angulo, C., et al. 1999, Nucl. Phys. A, 656, 3
Audi, G., Wapstra, A. H., & Thibault, C. 2003, Nucl. Phys. A, 729, 337
Endt, P. M. 1990, Nucl. Phys. A, 521, 1
Görres, J., Wiescher, M., & Rolfs, C. 1989, ApJ, 343, 365
Hale, S., et al. 2004, Phys. Rev. C, in press
Iliadis, C., Champagne, A. E., José, J., Starrfield, S., & Tupper, P. 2002, ApJS, 142, 105
José, J., Coc, A., & Hernanz, M. 1999, ApJ, 520, 347
José, J., & Hernanz, M. 1998, ApJ, 494, 680
José, J., Hernanz, M., Amari, S., Lodders, K., & Zinner, E. 2004, ApJ, 612, 414
Kovetz, A., & Prialnik, D. 1997, ApJ, 477, 356
Prantzos, N. 2004, A&A, 420, 1033
Rolfs, C. E., & Rodney, W. S. 1988, Cauldrons in the Cosmos (Chicago: Univ. Chicago Press)
Rowland, C., et al. 2002, Nucl. Instrum. Methods Phys. Res. A, 480, 610
Smith, D. M. 2004, NewA Rev., 48, 87
Starrfield, S., Truran, J. W., Wiescher, M. C., & Sparks, W. M. 1998, MNRAS, 296, 502
Vermeer, W. J., Pringle, D. M., & Wright, I. F. 1988, Nucl. Phys. A, 485, 380
Warner, B. 1995, Cataclysmic Variable Stars (Cambridge: Cambridge Univ. Press)